

## THE HUBBLE FLOW FROM BRIGHTEST CLUSTER GALAXIES

TOD R. LAUER<sup>1</sup>

Kitt Peak National Observatory, National Optical Astronomy Observatories, P.O. Box 26732, Tucson, AZ 85726

AND

MARC POSTMAN<sup>2</sup>

Space Telescope Science Institute<sup>3</sup>, 3700 San Martin Drive, Baltimore, MD 21218

Received 1992 July 22; accepted 1992 September 16

### ABSTRACT

We have imaged 114 Brightest Cluster Galaxies (BCG) from a full-sky sample of all Abell clusters within 15,000 km s<sup>-1</sup>. We present a BCG distance indicator based on reexamination of the Hoessel relationship between BCG metric luminosity and structure. The BCG Hubble diagram is consistent with a uniform Hubble flow over 0.01 ≤ *z* ≤ 0.05. We limit any variation in the *apparent* *H*<sub>0</sub> (measured globally from our location) to Δ*H*<sub>0</sub>/*H*<sub>0</sub> < 0.07 across the same volume. We use the Virgo BCG, NGC 4472, to calibrate the BCG Hubble diagram directly, independent of the Virgocentric infall pattern. For the observed distance to NGC 4472 of 14.4 Mpc, *H*<sub>0</sub> = 77 ± 8 km s<sup>-1</sup> Mpc<sup>-1</sup>. Alternatively, if NGC 4472 is at the Sandage & Tammann 21.9 Mpc distance to Virgo, then *H*<sub>0</sub> = 51 ± 5. The BCG Hubble constant on either the short or long system is consistent with Hubble constants measured on the same system within the local supercluster. Plausible high values of *H*<sub>0</sub> observed within the local supercluster therefore cannot be explained as biased measures of the true *H*<sub>0</sub> due to velocity anomalies induced by large-scale structure.

*Subject headings:* distance scale — large-scale structure of universe — galaxies: fundamental parameters

### 1. INTRODUCTION

A crucial step in measurement of the Hubble constant, *H*<sub>0</sub>, is identification of a scale beyond which noncosmological velocities are trivial compared to the Hubble flow. Turner, Cen, & Ostriker (1992) argue that *H*<sub>0</sub> as observed may strongly depend on the scale over which it is measured as a natural consequence of large-scale structure. It is now understood, for example, that the existence of a large-scale infall pattern associated with the Virgo cluster means that observation of the unbiased Hubble flow can only be contemplated at distances in excess of ~3000 km s<sup>-1</sup>.

Brightest Cluster Galaxies (BCG), or more precisely BCG that are also elliptical or cD galaxies, offer the best observation of the Hubble flow out to cosmologically interesting scales. BCG are bright and can be observed out to the Hubble radius, and their luminosities are constant with an impressively small dispersion. Sandage (1972), and Sandage & Hardy (1973) used BCG to argue that the Hubble flow is linear and shows no evidence of variation in *H*<sub>0</sub> or even modest peculiar velocities at low redshift. More recently, Sandage & Tammann (1990) used the BCG Hubble diagram as one of three methods for inferring a far-field *H*<sub>0</sub> from the Virgo-based distance scale.

In this *Letter* we present the initial results from our reinvestigation of the BCG distance scale, which includes richer sampling and complete all-sky observations of Abell clusters within 15,000 km s<sup>-1</sup>. Our goal is to detect the reflex motion of the Local Group with respect to the Abell cluster inertial frame. Analysis of the Local Group velocity as well as exten-

sive description of the BCG observations will be presented elsewhere (Lauer & Postman 1992, hereafter LP92), for now we examine use of BCG to look for any evidence that the *apparent* global value of *H*<sub>0</sub> measured about our location changes as a function of depth.

### 2. OBSERVATIONS AND ANALYSIS

#### 2.1. Sample Selection and Observations

We selected for possible observation all 151 Abell (1958) and Abell, Corwin, & Olowin (1989, ACO) clusters with observed or estimated redshifts within 15,000 km s<sup>-1</sup> to construct a volume-limited sample of BCGs. For clusters with fewer than 3 measured redshifts, new observations were obtained by us at CTIO for southern ACO clusters and by Huchra (1992) in the north for 17 clusters. At the minimum, we have acquired velocities for at least three galaxies per cluster including the BCG (51% of the clusters have measurements for 10 or more member galaxies). A crucial part of our program was a full reinvestigation of use of BCG as distance indicators, beginning with identification of candidate BCG from sky survey plates. Final BCG identification was not made until CCD images were obtained for all BCG candidates in a given cluster. Redshift data were also used to guide BCG selection. Of the original 151 clusters, 125 were ultimately found to have *z* ≤ 0.05; four had a spiral BCG, three were not imaged, A400 and A3555 had anomalously faint BCG, A3627 was excluded due to its extremely low galactic latitude, and A426 was excluded given the well-known A-type spectrum of its BCG, NGC 1275, leaving us with 114 BCGs. The redshifts used in the Hubble diagram represent the best average of all material available for a given cluster (see LP92).

Photometric CCD observations of all BCG were obtained using the KPNO 4 m and 2.1 m telescopes, and the CTIO 1.5 m telescope between 1989 November and 1991 April. Images were obtained in the Kron-Cousins *R*<sub>c</sub> band, which is our

<sup>1</sup> Visiting Astronomer Cerro Tololo Inter-American Observatory, National Optical Astronomy Observatories. NOAO is operated by the Association of Universities for Research in Astronomy, Inc., under cooperative agreement with the National Science Foundation.

<sup>2</sup> Visiting Astronomer, Kitt Peak National Observatory and Cerro Tololo Inter-American Observatory.

<sup>3</sup> STScI is operated by AURA, Inc., under contract to the National Aeronautics and Space Administration.

primary choice for the bandpass of the photometric distance indicator, and the standard Johnson  $B$  band, which is used to investigate color-magnitude relationships as well as verifying the interstellar extinction corrections. As a variety of CCDs were used, a large sample of galaxies were observed in common between the various runs to assure that all observations reduce to the same photometric zero point. The random photometric error for any BCG is 0.01 mag. For the analysis that follows, we have applied a  $K$ -correction, and use the Burstein & Heiles (1984) extinction estimates.

In a majority of cases the BCG was either a “multiple-nucleus” system or was significantly contaminated by another cluster galaxy projected along the line of sight. The reduction procedure adopted for all systems was to isolate the primary BCG component by use of the multi-isophote decomposition photometry software of Lauer (1986). The final photometric material for a given BCG consists of the modeled galaxy light integrated through a geometric series of apertures.

## 2.2. Distance Indicator

The absolute magnitudes of BCG,  $L_m$ , measured in apertures of fixed metric size,  $r_m$ , are constant to first order. Further, the random scatter in  $L_m$ ,  $\sigma_L$ , depends only weakly on the particular aperture choice. For example, Hoessel (1980) found  $\sigma_L = 0.34$  mag, using  $r_m = 9.6 h^{-1}$  kpc. Some of the scatter in  $L_m$  may be due to weak BCG luminosity correlations with cluster richness and Bautz-Morgan type (Sandage 1972). Hoessel (1980) also observed a relationship between  $L_m$  and  $\alpha \equiv d \log L_m / d \log r |_{r_m}$ . In essence, an  $L_m - \alpha$  relationship can be thought of as a sort of magnitude-radius relationship for BCG. Use of  $\alpha$  to reduce scatter in  $L_m$  is attractive since it is objectively defined and is a direct product of the galaxy photometry, whereas cluster properties such as richness and Bautz-Morgan type are highly subjective and remain problematic even with copious velocity observations of cluster members. Since BCG are extended sources, knowledge of  $\alpha$  is also required to relate  $\sigma_L$  to corresponding distance errors; which for small  $\sigma_L$  are  $\sigma_D = \sigma_L / (2 - \alpha)$  (Gunn & Oke 1975).

We find a clear relationship between  $L_m$  and  $\alpha$  for our BCG sample, as shown in Figure 1. For small  $\alpha$  the relationship appears to have a constant linear slope, but it flattens out toward larger  $\alpha$ ; a parabolic fit appears adequate to match this nonlinearity and produces significantly smaller residuals than does a purely linear fit. In general, we have adopted  $r_m = 10 h^{-1}$  kpc, or in angular terms as a function of redshift (for  $q_0 = 0.5$ ),

$$\theta_m = 0''.3440(1+z)/[1 - (1+z)^{-1/2}]. \quad (1)$$

The choice of  $r_m$  is based on exploring the scatter,  $\sigma_L$ , about a quadratic relationship in  $\alpha$  fitted to the observed  $L_m$  as a function of  $r_m$ ; the final  $L_m - \alpha$  fit is also shown in Figure 1. A broad minimum in  $\sigma_L$  occurs at about  $r_m = 10 h^{-1}$  kpc; for our sample and aperture choice we get  $\sigma_L = 0.25$  mag. We find that use of BCG central velocity dispersions further reduces  $\sigma_L$  to 0.16 mag (LP92), but central dispersions are currently available for only a fraction of our sample and are thus not used in the present Hubble diagram.

Implicit in Figure 1 is a relationship between distance and recession velocity of the galaxy clusters. At present we have assumed that the Local Group is at rest with respect to the Abell cluster frame. Since our sample covers the full celestial sphere (but for the zone of avoidance implicit in the Abell catalog), to first order any dipole pattern present in the residuals due to the reflex motion of the Local Group will

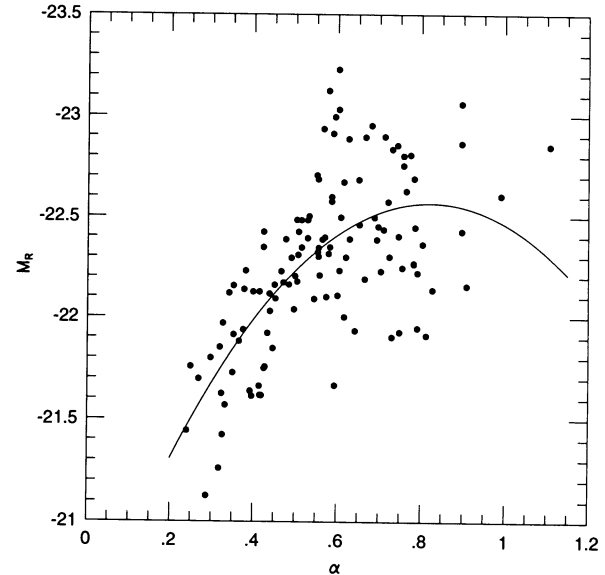


FIG. 1.—The  $L_m - \alpha$  relationship for the BCG sample. The mean fit to the  $R_c$  band  $r_m = 10 h^{-1}$  kpc absolute metric luminosities as a function of  $\alpha$  is also shown. Velocities relative to the Local Group and  $H_0 = 77 \text{ km s}^{-1} \text{ Mpc}^{-1}$  have been assumed.

average to zero, and will not bias the global Hubble diagram. We note, however, that Turner et al. (1992) argue that bulk flows within a volume may also have an associated *monopole* term that may bias the Hubble constant derived from the volume *independent* of complete sampling of the dipole; such an effect would be visible as differences in the Hubble constants measured interior and exterior to the radius at which the bulk flow converges.

## 3. BCG HUBBLE DIAGRAM

### 3.1. Linearity of Hubble Diagram

In Figure 2 we plot the apparent magnitudes of our BCG sample as a function of velocity to produce the BCG Hubble diagram. We have removed the effects of the  $L_m - \alpha$  relationship by subtracting the mean  $\alpha$ -dependent luminosity offset

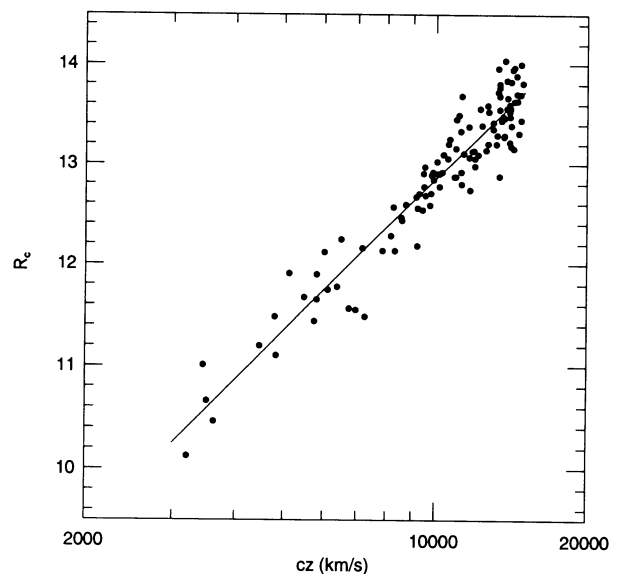


FIG. 2.—The BCG magnitude-redshift relationship corrected by the  $L_m - \alpha$  relationship.

with respect to  $\alpha = 0.5$ . The Hubble diagram shows little apparent deviation from linearity; a fit of a linear magnitude-redshift relationship gives

$$R_c = 20.203 \pm 0.027 + (0.996 \pm 0.030)5 \log(z). \quad (2)$$

This result is strongly weighted by BCG near the high-velocity limit, given that the BCG sample is volume limited; however, the essentially unit slope with 3% error implies global  $\Delta H_0/H_0 < 0.07$  from 3000 km s<sup>-1</sup> to 15,000 km s<sup>-1</sup> [we calculate  $\Delta H_0/H_0 = \Delta R_c/(2 - \alpha) \Delta \log(z)$ ]. An important question is how variations in  $H_0$  due to the effects of large-scale structure would be revealed in the BCG Hubble diagram. Turner et al. (1992) present distributions of measured  $H_0$  at various survey depths based on a large ensemble of simulations of various models for the formation of large-scale structure, showing that the variance of  $H_0$  is a strong function of scale, but do not explicitly address what the Hubble diagrams would look like in models where the local and far-field expansion rates strongly differ. The linearity of equation (2) and the unit slope are sensitive to changes in  $H_0$  with depth, however, and offer strong constraints that such changes must be small.

Apart from any gross variation of  $H_0$  over the BCG sample, we might ask whether there are any significant variations over small scales. Just  $\sigma_L = 0.25$  mag alone implies that variation in  $H_0$  will be limited to 16%, on the assumption that *all* of the scatter in Figure 1 is due to peculiar velocities (assuming typical BCG  $\alpha \approx 0.5$ ). We plot the binned residuals with respect to equation (2) as a function of depth in Figure 3, expressed as  $\Delta H_0/H_0$  as a search for variations in  $H_0$  with redshift. What we are asking is if the BCG in any spherical shell 3000 km s<sup>-1</sup> thick centered on our location show an expansion rate different from the entire sample average (we show shells at 1500 km s<sup>-1</sup> intervals to sample properly any structure present). With this binning, two shells near the low redshift end fall on opposite sides of the mean relationship by  $\Delta H_0/H_0 \approx 0.06 \pm 0.05$ . A fit to the 27 BCG with  $3000 \leq cz \leq 9000$  km s<sup>-1</sup> gives the slope in equation (2) as  $0.882 \pm 0.084$ , implying  $\Delta H_0/H_0 = -0.18 \pm 0.13$  over the same interval. The significance of this result is hardly strong, however, and as noted above, residuals in the  $L_m - \alpha$  relationship correlate with central velocity dispersion (LP92), which may explain much of the variation in Figure 3. Only 10 of the 27 BCG have measured velocity dispersions (vs. 44 for the full sample), but examination of the residuals suggests that there

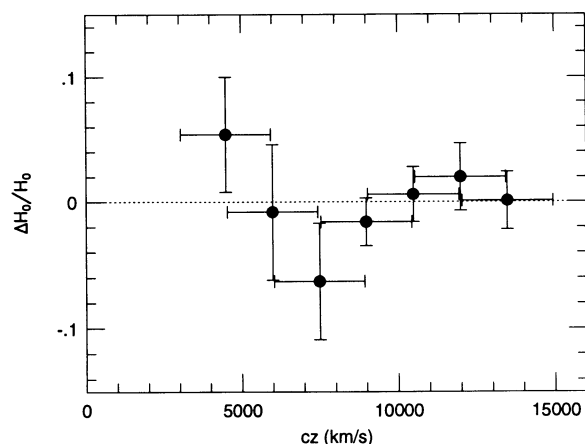


FIG. 3.—Residuals with respect to the mean Hubble flow shown in Fig. 2 are shown in bins 3000 km s<sup>-1</sup> wide in terms of the implied  $\Delta H_0/H_0$ . Bins are separated by 1500 km s<sup>-1</sup>.

may be real differences in the intrinsic properties of the BCG between the two bins with the largest deviations in Figure 3. For now, from equation (2) and Figure 3, we only conclude that  $H_0$  measured globally is constant to  $\pm 7\%$  from 3000 km s<sup>-1</sup> to 15,000 km s<sup>-1</sup>.

### 3.2. Absolute Calibration of the Hubble Diagram

Calibration of the BCG distance scale itself would provide the best measure of the Hubble constant well removed from local velocity anomalies, as well as providing a check on whether  $H_0$  varies between the local and far field. Unfortunately, the three methods favored for measuring distances to elliptical galaxies, planetary nebula luminosity functions, surface brightness fluctuations, and globular cluster luminosity functions all are extremely difficult to use from the ground for even the lowest redshift members of the BCG sample. We can attempt a provisional calibration, however, using the distance to NGC 4472, the brightest galaxy in the Virgo cluster. Virgo is not formally an Abell cluster, but our application of the Abell (1958) cluster selection criteria to galaxies assumed to be Virgo members argues that it would be a richness class 0 to 1 member of the Abell catalog if it were at a large enough distance to fit within Abell's maximum angular size cutoff.

All three methods listed above have been used to estimate the distance to NGC 4472. The Tonry, Ajhar, & Luppino (1990) surface brightness fluctuation distance recalibrated by Tonry (1991) gives the distance as  $14.3 \pm 0.4$  Mpc. The planetary nebula luminosity function distance of Jacoby, Ciardullo, & Ford (1990) recalibrated for a new distance to M31 (see Jacoby et al. 1992) also gives  $14.3 \pm 0.6$  Mpc. The globular cluster luminosity function gives a larger distance of  $17.5 \pm 2.1$  Mpc, but is also less accurate (Harris et al. 1991). The error-weighted average of all three measures yields a distance of 14.4 Mpc. In passing, we note that even if NGC 4472 is slightly in the foreground of the Virgo core at 16.0 Mpc (Jacoby et al. 1992), NGC 4472 still remains brighter than NGC 4486, the second-ranked Virgo galaxy.

Photometric information on NGC 4472 comes from a deep KPNO 4 m V-band CCD image kindly provided by Dr. George Jacoby. Calibration was provided by a summary of all available photometry (D. Burstein, private communication), and we have assumed  $V - R_c = 0.62$  (LP92) and zero interstellar reddening. Absolute calibration of the BCG Hubble diagram comes from finding the metric aperture size for an assumed distance to NGC 4472 that places it on the mean  $L_m - \alpha$  relationship shown in Figure 1. The primary source of internal error in this procedure is the 0.25 mag dispersion in  $L_m$  alone for the BCG sample, or 0.16 mag when central velocity dispersions are available. For NGC 4472 Whitmore, McElroy, & Tonry (1985) give  $\sigma = 315$  km s<sup>-1</sup> this implies that NGC 4472 will fall on the bright side of the mean  $L_m - \alpha$  relation by 0.05 mag (LP92). With this adjustment,  $r_m = 10 h^{-1}$  kpc corresponds to  $\theta_m = 185''$  at NGC 4472, giving  $R_c = 8.25$  and  $\alpha = 0.54$ ; the implied distance error is 10%, assuming the basic 0.16 mag dispersion increased by  $2/(2 - \alpha)$ . For a distance to NGC 4472 of 14.4 Mpc,  $\theta_m$  corresponds to  $r_m = 13.0$  kpc implying that the BCG  $H_0 = 77 \pm 8$  km s<sup>-1</sup> Mpc<sup>-1</sup>.

The present BCG  $H_0$  depends purely on methods used to measure distances to elliptical galaxies and the BCG Hubble diagram, but does not depend on uncertainties in the distance of NGC 4472 with respect to Virgo, Virgocentric infall, or any other recognizable velocity anomaly; measurement of distances to other BCG can be used to refine this value further. On the other hand, we note that the methods used to derive the

NGC 4472 distance are controversial and that the BCG Hubble diagram can be calibrated on the long-distance scale as well. Sandage & Tammann (1990) do not present a distance to NGC 4472 per se, but derive a mean distance to Virgo of 21.9 Mpc. If NGC 4472 is assigned to this distance, this gives the BCG  $H_0 = 51 \pm 5$ , essentially identical to the BCG  $H_0$  presented by Sandage & Tammann (1990).

Regardless of which of the short or long-distance scale calibrations is correct, in either system the BCG  $H_0$  nicely matches measurements of  $H_0$  obtained interior to the BCG sample. Jacoby et al. (1992), for example, derive a distance to Virgo of  $16.0 \pm 1.7$  Mpc from a weighted average of several methods that include those used to estimate the distance to NGC 4472, and then use the relative distance of Coma to Virgo of  $5.6 \pm 0.5$  to avoid local velocity anomalies, and find  $H_0 = 80 \pm 11$ . This can be compared to  $H_0 = 73\text{--}86$  derived directly from the same Virgo distance with infall corrections in the range  $100\text{--}300 \text{ km s}^{-1}$  (Huchra 1988). Both measures nicely agree with the BCG  $H_0 = 77 \pm 8$ ; we thus conclude that there is at present no evidence that  $H_0$  measured globally from our location varies significantly over  $z < 0.05$  once the Virgocentric infall pattern is accounted for.

#### 4. SUMMARY

We have presented the BCG Hubble diagram based on a full-sky sample of all Abell and ACO clusters within  $15,000 \text{ km s}^{-1}$ . This survey is the most photometrically homogeneous and

most densely sampled BCG survey within this volume to date, and it provides important new constraints on the apparent variations of  $H_0$  on large scales. We find that the slope of the relationship between BCG magnitude and redshift is as expected for a uniform Hubble flow unaffected by any large-scale velocity anomalies. While it's clear that there are many locations within the local supercluster where an observer would see a biased Hubble flow measured within the surrounding volumes and that there are lines of sight that for observers here that are strongly affected by bulk motions and infall, our results suggest that biases in  $H_0$  measured globally do not exist for an observer at our location, once one goes beyond the effects of Virgo. On the other hand, one might wonder if the whole volume interior to  $15,000 \text{ km s}^{-1}$  is itself uniformly biased, but the BCG Hubble diagram presented by Sandage & Hardy (1973), remains linear out to twice this distance. The uniformity of the Hubble flow thus argues against the idea that the apparent high values of  $H_0$  observed within the local supercluster are purely an anomaly of large-scale flows. The path to removing any uncertainty in the true  $H_0$  remains with understanding the local distance scale.

We thank Dr. George Jacoby and Dr. Sandra Faber for useful discussions. We thank Dr. John Huchra and Dr. Ann Zabludoff for providing redshift data in advance of publication.

#### REFERENCES

- Abell, G. O. 1958, *ApJS*, 3, 211  
 Abell, G. O., Corwin, H. G., & Olowin, R. P. 1989, *ApJS*, 70, 1  
 Burstein, D., & Heiles, C. 1984, *ApJS*, 54, 33  
 Gunn, J. E., & Oke, J. B. 1975, *ApJ*, 195, 255  
 Harris, W. E., Allwright, J. W. B., Pritchet, C. J., & van den Bergh, S. 1991, *ApJS*, 76, 115  
 Hoessel, J. G. 1980, *ApJ*, 241, 493  
 Huchra, J. P. 1988, in *The Extragalactic Distance Scale*, ed. S. van den Bergh & C. J. Pritchet (Provo: Brigham Young Univ), 257  
 ———. 1992, private communication  
 Jacoby, G. H., Ciardullo, R., & Ford, H. C. 1990, *ApJ*, 356, 332  
 Jacoby, G. H., et al. 1992, *PASP*, 104, 599  
 Lauer, T. R. 1986, *ApJ*, 311, 34  
 Lauer, T. R., & Postman, M. 1992, in preparation (LP92)  
 Sandage, A. 1972, *ApJ*, 178, 1  
 Sandage, A., & Hardy, E. 1973, *ApJ*, 183, 743  
 Sandage, A., & Tammann, G. A. 1990, *ApJ*, 365, 1  
 Tonry, J. L. 1991, *ApJ*, 373, L1  
 Tonry, J. L., Ajhar, E. A., & Luppino, G. A. 1990, *AJ*, 100, 1416  
 Turner, E. L., Cen, R., & Ostriker, J. P. 1992, *AJ*, 103, 1427  
 Whitmore, B. C., McElroy, D. B., & Tonry, J. L. 1985, *ApJS*, 59, 1